

A potent chemotherapeutic strategy in prostate cancer:

S-(methoxytrityl)-L-cysteine, a novel Eg5 inhibitor

Naidong Xing^{1,2}, Sentai Ding^{1,2}, Ryoichi Saito¹, Koji Nishizawa¹, Takashi Kobayashi¹,
Takahiro Inoue¹, Shinya Oishi³, Nobutaka Fujii³, Jiajv Lv², Osamu Ogawa^{1,*} and
Hiroyuki Nishiyama¹

¹Department of Urology, Kyoto University, Graduate School of Medicine, Kyoto,
Japan

²Department of Urology, Provincial Hospital affiliated to Shandong University, Jinan,
Shandong, China

³Graduate School of Pharmaceutical Sciences, Kyoto University, Kyoto, Japan

***Correspondence:** Dr Osamu Ogawa, Department of Urology, Kyoto University,
Graduate School of Medicine, 54 Shogoin Kawaharacho, Sakyo-ku, Kyoto 606-8507,
Japan. Tel: 81-75-751-3325. Fax: 81-75-761-3441. E-mail:
ogawao@kuhp.kyoto-u.ac.jp

Running title: S(MeO)TLC for treatment of prostate cancer

Abstract

Docetaxel-based combination chemotherapy remains the predominant treatment for castration-resistant prostate cancer. However, taxane-related drug resistance and neurotoxicity have prompted us to develop substitute treatment strategies. Eg5 (kinesin spindle protein), which is crucial for bipolar spindle formation and duplicated chromosome separation during the early phase of mitosis, has emerged as an attractive target for cancer chemotherapy. The aim of this study was to investigate the anticancer efficacy of *S*-(methoxytrityl)-L-cysteine [S(MeO)TLC], a novel Eg5 inhibitor in prostate cancer. Eg5 expression was examined in human prostate cancer cell lines and tissue microarrays constructed from clinical specimens. Anti-proliferative activity of S(MeO)TLC in prostate cancer cells was assessed by a cell viability assay. The anticancer effect and inhibitory mechanism of S(MeO)TLC in prostate cancer cells was further explored by Hoechst staining, flow cytometry and immunofluorescence. In addition, the antitumor effect of S(MeO)TLC on subcutaneous xenograft models was assessed. Eg5 expression was identified in PC3, DU145 and LNCaP cells. More than half of prostate cancer clinical specimens displayed Eg5 expression. S(MeO)TLC exhibited more powerful anticancer activity in prostate cancer cells compared with the other four Eg5 inhibitors tested. S(MeO)TLC induced cell death after arresting dividing cells at mitosis with distinct monopolar spindle formation. S(MeO)TLC exhibited its significant inhibitory activity ($P < 0.05$) on subcutaneous xenograft models also through induction of mitotic arrest. We conclude that Eg5 is a good target for prostate cancer chemotherapy, and

S(MeO)TLC is a potent promising anticancer agent in prostate cancer.

Keywords: Eg5 protein, prostate cancer, *S*-(methoxytrityl)-L-cysteine

Introduction

Prostate cancer is one of the most commonly diagnosed malignancies and the second highest cause of cancer death in American men, with an estimated 27 360 patients dying of castration-resistant prostate cancer (CRPC) in 2009 ¹. Furthermore, in recent years, there has been a more rapid increase in the incidence and mortality rates in Asian countries ². Androgen deprivation therapy (ADT), including surgical orchiectomy and luteinizing hormone-releasing hormone agonists are the primary treatments for patients with advanced prostate cancer. These patients respond initially to ADT within 1–2 years, but eventually they progress to CRPC. Eventually CRPC develops followed by ADT after 1 to 2 years' response time ³. Combination chemotherapy based on docetaxel is the standard treatment for patients with CRPC ^{4,5}. However, no standard treatment options are established once patients with CRPC progress. Moreover, docetaxel as an anti-microtubule drug has its limitations, including drug resistance and side effects caused by drug-binding site mutations on β -tubulin ⁶, overexpression of P-glycoprotein ⁷ and β -tubulin ⁸, and neurotoxicity ⁹. Therefore, there is an urgent need to develop alternative treatment strategies.

Eg5, also known as kinesin spindle protein ¹⁰, is a member of the kinesin-5 motor proteins, and plays a crucial role in bipolar spindle formation and duplicated chromosome separation during the early phase of mitosis ^{11,12}. Inhibition of Eg5 can

arrest dividing cells in mitosis followed by cell death, without affecting the function of interphase microtubules¹³, thus offering an encouraging alternative to microtubule-targeted cancer chemotherapy. The first Eg5-specific inhibitor was identified in 1999 on the basis of phenotype-screening, and named monastrol because it can induce monoastrol spindle formation¹². Inactivation of Eg5 cannot cause peripheral neuropathy because of Eg5 localization to mitotic spindle microtubules but not to interphase microtubules¹⁴. Eg5 inhibitors can overcome multidrug resistance to taxanes caused by overexpression of P-glycoprotein because Eg5 cannot be transported out of cells by P-glycoprotein^{15,16}. *S*-(methoxytrityl)-L-cysteine [S(MeO)TLC]¹⁷, a derivative of *S*-trityl-L-cysteine (STLC)¹⁸, can specifically inhibit Eg5, as does STLC¹⁹, and induce monopolar mitotic spindle formation, but it is more than 10 times as potent as STLC¹⁷. Meanwhile, the functionalized indoles, such as KPYC10665 (2-(trifluoromethyl)-9*H*-carbazole), KPYC10666 (2-(*tert*-butyl)-9*H*-carbazole) and KPYC10728 (7-(trifluoromethyl)-9*H*-pyrido[3,4-*b*]indole), which are synthesized by one-pot *N*-arylation-oxidative biaryl coupling of anilines and phenyl triflates²⁰, are also potent Eg5 inhibitors²¹.

In our previous study, S(MeO)TLC displayed its potent anticancer efficacy in bladder cancer *in vitro* and *in vivo*²². In the present study, we examined Eg5 expression in prostate cancer cells. We also analyzed the relationship between Eg5 expression in clinical samples and clinicopathological characteristics. We assessed the potent anticancer efficacy of S(MeO)TLC both *in vitro* and *in vivo*.

Materials and methods

Cell culture and drug compounds

The prostate cancer cell lines PC3, DU145 and LNCaP were obtained from the American Type Culture Collection (ATCC; Rockville, MD, USA). PC3^{Luc} cell line was also constructed and used. PC3 cells were lipofected with pGL3-control plasmid vector (firefly luciferase gene; Promega, Madison, WI, USA) and pSV2Neo plasmid (a vector for neomycin resistance; ATCC), as described previously²³. The clone that stably expressed strongest luciferase activity was designated PC3^{Luc}. The cells were routinely propagated in RPMI 1640 supplemented with 10% fetal bovine serum and 1% penicillin/streptomycin, and incubated at 37°C with a humidified 5% CO₂ atmosphere.

Five Eg5 inhibitors were used in our study. KPYC10665, KPYC10666 and KPYC10728 were synthesized in our institute, and STLC and S(MeO)TLC were purchased from Bachem (Bubendorf, Switzerland). All compounds were dissolved in DMSO and stored at –20°C.

Eg5 expression in prostate cancer tissue microarrays (TMAs) and cells

After obtaining approval from the Institutional Review Board at Kyoto University Hospital and informed consent, a total of 80 archival specimens of clinically localized prostate cancer patients who underwent radical prostatectomy at our institute were

used in the study. TMAs were constructed from these specimens as previously described²⁴. Standard indirect immunoperoxidase assays using primary anti-Eg5 rabbit antibody (1:300; Cytoskeleton, Denver, CO, USA) were performed to detect Eg5 antigen. Eg5 immunostaining was considered positive if the cytoplasm of $\geq 5\%$ cancer cells showed weak or greater intensity. Ki67 labeling index was determined as previously described²⁴. All pathological evaluations were performed independently by two of the authors (N.X. and T.K.). Assessment of Gleason grading and cancer staging were based on standard hematoxylin and eosin (H&E) staining and clinical data according to the 2002 American Joint Committee on Cancer TNM classification and the Japanese General Rules for Clinical and Pathological Studies on Prostate cancer (third edition)^{25,26}. The correlation between clinicopathological characteristics and Eg5 immunohistological expression was analyzed statistically.

Eg5 expression in prostate cancer cell lines was determined by western blot analysis using standard methods as described previously²⁷. Briefly, 25 μg protein extracts were added to each lane and separated by SDS-PAGE (30 mA for 120 min), then blotted onto a polyvinylidene difluoride membrane (16 V for 120 min). After incubated with 5% non-fat dry milk for an hour at room temperature, membranes were incubated with rabbit primary antibody (1:1 000; Cytoskeleton) for Eg5 detection and anti- β -actin mouse antibody (1:20 000; Abcam, Cambridge, UK), which was employed as an internal control. After incubation with corresponding horseradish peroxidase-conjugated secondary antibodies (anti-rabbit, 1:25 000; anti-mouse, 1:10 000), ECL solution (GE healthcare, Buckinghamshire, UK) was applied to react with

the membranes and reactive bands were imaged by a PhosphorImager (GE Healthcare, Buckinghamshire, UK).

Cell viability assay

Cell viability was determined using the 3-(4, 5-dimethylthiazol-2-yl)-2, 5-diphenyltetrazolium bromide (MTT) assay, as described previously²⁷. Cells were grown in 96-well plates at a density of 2.5×10^3 cells per well and incubated for 24 h. After that, cells were administered varying concentrations of Eg5 inhibitors, or DMSO alone as a control, for additional 72 h incubation. The concentrations of 50% cell growth inhibition (IC_{50}) were assessed according to the dose–response curve.

Trypan blue staining was also used to assess the percentage of viable cells, as described previously²⁷.

Flow cytometry assay and Hoechst staining

To assess the cell cycle distribution, DNA content of PC3 cells treated with S(MeO)TLC or vehicle was stained by 7-amino-actinomycin D (BD Biosciences, SanDiego, CA, USA) and assayed by flow cytometry, as described previously²⁸. At least 10 000 cells, including floating and attached cells, were collected and analyzed by using a FACSCalibur flow cytometer and CellQuest software (BD Biosciences).

Nuclei of the control and treated cells were stained with 1 mM Hoechst 33342 solution (Wako, Osaka, Japan). The typical morphological changes of apoptotic cells, such as condensation and fragmentation of the nuclei, were visualized and identified with a fluorescence microscope (Biozero; Keyence, Osaka, Japan).

Immunocytofluorescent staining

To observe microtubules, 1×10^5 PC3 cells treated with S(MeO)TLC for 16 h or vehicle alone were fixed and incubated with rabbit anti- α -tubulin primary antibody (Cell Signaling Technology, Boston, MA, USA), followed by tetramethylrhodamine-isothiocyanate-conjugated polyclonal swine anti-rabbit IgG (Dako, Glostrup, Denmark). Vectashield Hard Set Mounting Medium with 4,6-diamidino-2-phenylindole (DAPI; Vector Laboratories, Burlingame, CA, USA) was added for counterstaining of nuclei. Fluorescent microscopic images were acquired using a fluorescence microscope (Biozero; Keyence, Osaka, Japan), and false color (green) was used for nuclei.

Prostate cancer tumor xenograft studies

Exponentially growing PC3^{luc} cells (5×10^6 cells for one tumor) suspended in 200 μ L PBS were injected subcutaneously into both flanks of 6-week-old male nude mice (BALB/c AJcI-nu/nu; Japan CLEA, Osaka, Japan). The tumor volume was computed as: volume = length \times width² \times 0.5236. When the tumor volume reached ~ 70 mm³, 12 mice were randomly divided into three groups and treated by daily intraperitoneal injection with 10 or 20 mg kg⁻¹ S(MeO)TLC or vehicle alone for 5 days. Tumor volume and mouse body weight were monitored every other day. On the day 24 after the first treatment, all mice were sacrificed. Tumors were excised, weighed, formalin-fixed and H&E-stained for histological analysis. Tumors from two mice in

each group that were sacrificed at 24 h after 5 days treatment with S(MeO)TLC or vehicle alone were also formalin-fixed and analyzed histologically using H&E staining. Mice were kept under specific pathogen-free conditions, and all animal experiments were approved by the Committee on Animal Research at our institute.

Statistical analysis

SPSS 16.0 software (Chicago, IL, USA) was utilized for statistical analysis. Statistical significance was defined as $P < 0.05$. Two-tailed tests were used. In analysis of TMAs, the differences in age, prostate-specific antigen (PSA), Ki-67 labeling index (Ki67 LI) between Eg5-positive and -negative groups were analyzed using the Mann–Whitney U test. The correlation of Eg5 expression and Gleason score, pathological T stage, and positive surgical margin (PSM) was conducted by χ^2 test or Fisher exact test. The mean subcutaneous tumor volumes, tumor weights and body weights between groups at the end of observation were compared using one-way ANOVA. The least squares method was used to evaluate the difference between each two groups when ANOVA was significant ($P < 0.05$).

Results

Expression of Eg5 in prostate cancer

We evaluated Eg5 expression in prostate cancer cell lines using western blot analysis. Eg5 expression was identified in all three cell lines, LNCaP, PC3 and DU145 (Figure 1A). We investigated Eg5 expression in prostate cancer clinical samples by

immunohistochemistry using TMAs. Eg5 immunostaining was mainly observed in the cytoplasm (Figure 1B). As shown in Table 1, more than half (55.6%, 44/80) of prostate cancer clinical specimens exhibited Eg5 expression. Statistical analysis revealed that Eg5 expression was significantly associated with Ki67 LI ($P = 0.004$), although there were no significant relationships between Eg5 expression and the other clinicopathological parameters ($P > 0.05$).

Anti-proliferative activity of Eg5 inhibitors against prostate cancer cells

In our study, the anti-proliferative activity of five Eg5 inhibitors on prostate cancer cells was assessed using MTT assay. As shown in Figure 2A and Table 2, the IC_{50} (95% CI) of KPYC10665, KPYC10666, KPYC10728, STLC and S(MeO)TLC on PC3 cells was 6.54 (6.13–6.98) μ M, 6.78 (6.21–7.37) μ M, 1.44 (1.23–1.67) μ M, 1.10 (0.93–1.32) μ M, and 0.107 (0.081–0.137) μ M, respectively. All these five Eg5 inhibitors had anticancer effects on PC3 cells. S(MeO)TLC exhibited the most efficient anticancer activity, with an IC_{50} that was at least 10-fold lower than that of the other agents. Similar results were obtained in DU145 cells (Table 2). S(MeO)TLC also showed a strong inhibitory effect on LNCaP cells (data not shown). Trypan blue staining (Figure 2B) showed that viability of PC3 cells treated with 500 nM S(MeO)TLC for 48 h decreased significantly in comparison with the controls (t test, $P < 0.01$).

MTT assay and trypan blue staining verified that Eg5 inhibitors can substantially inhibit prostate cancer cell proliferation and promote cell death. To explore the

mechanism by which S(MeO)TLC exerts its anti-proliferative activity in prostate cancer cell lines, the cell cycle distribution analysis was performed by flow cytometry (Figure 3A and 3B). Compared with the control, the G2/M phase of PC3 cells after treatment with 500 nM S(MeO)TLC increased considerably. The percentage of mitotic cells reached a peak after 16 h of treatment (G2/M phase cells, $92.1 \pm 4.3\%$). After mitotic arrest, the proportion of apoptotic cells (subG1) increased to $2.3 \pm 0.5\%$ and $15.5 \pm 2.4\%$, after 24 h and 48 h treatment, respectively. Hoechst 33342 staining revealed that a majority of monopolar spindle cells arrested in mitosis were observed at 16 h after treatment with S(MeO)TLC, and typical nuclear morphological changes of apoptotic cells with condensation and fragmentation of the nuclei were also identified at 48 h after treatment (Figure 3C). Cells with apoptotic morphology increased significantly after 48 h treatment (Figure 3D, $P < 0.05$). The distinctive monopolar spindle morphology with a rosette-like phenotype induced by S(MeO)TLC was further visualized by immunofluorescence assay (Figure 3E), and such cells also increased significantly after 16 h treatment (Figure 3F, $P < 0.01$). Collectively, these data confirmed that the anti-proliferative activity of S(MeO)TLC in prostate cancer cells is induced by mitotic arrest followed by apoptosis.

Efficacy of S(MeO)TLC in the prostate cancer xenograft model

Our previous study showed that S(MeO)TLC ($400 \mu\text{g kg}^{-1}$ to 20mg kg^{-1}) exhibited significant anticancer efficacy ($P < 0.05$) in the human bladder cancer (KU7) subcutaneous xenograft models in a dose-dependent manner²². Also, there was no

significant difference ($P > 0.05$) in tumor growth between the 20 and 30 mg kg⁻¹ groups. Among the five Eg5 inhibitors tested, S(MeO)TLC was the most effective one for the inhibition of KU7 xenograft tumor growth, and the IC₅₀ of S(MeO)TLC on KU7 and PC3 cells was almost the same. Therefore, in our present study, we only evaluated the anticancer efficacy of S(MeO)TLC in PC3^{luc} subcutaneous xenograft models using doses of 10 and 20 mg kg⁻¹ and an equal amount of vehicle as a control. As shown in Figure 4A, on day 24 after the first treatment, S(MeO)TLC considerably inhibited subcutaneous tumor growth in a dose-dependent manner ($P < 0.05$). At the end of the observation, we also compared mean final tumor weights between treatment and control groups. The data confirmed that difference in the mean final tumor weights between the two groups was statistically significant (Figure 4B, $P < 0.05$). No obvious body weight changes and other toxic events such as motor disorder and mortality were seen in any group (data not shown). The microscopic appearance of the tumors is shown in Figure 4C. Characteristic monopolar spindle mitotic cells were observed in H&E-stained tumors from the S(MeO)TLC-treated mice, but not in the control group (Figure 4C).

Discussion

Cancer cells enter into the cell cycle and undergo uncontrolled mitosis permanently, which results in unlimited tumor growth. Thus, drugs that interfere with mitosis have emerged as the most successful chemotherapeutic agents in clinical use today^{29,30}. Among them, anti-microtubule agents, including taxanes and vinca alkaloids that

disturb microtubule dynamics of mitosis, represent the most effective anticancer drugs^{29,30}. Given the success of taxanes in cancer therapy by perturbing mitosis, Eg5, which is more highly expressed in proliferating tissues during mitosis³¹, is considered as an attractive target for cancer chemotherapy.

Accumulating evidence also indicates that Eg5 inhibition is especially relevant in the treatment of CRPC. In addition to sharing the target molecules with taxanes, Eg5 inhibitors can also exhibit powerful anticancer activity in taxol-resistant cancer cells, and they can overcome taxane resistance¹⁶. In addition, they can overcome taxane-related peripheral neurotoxicity^{13,32}. It has been also reported that, in androgen-independent progression of prostate cancer cells, the androgen receptor distinctly upregulates M-phase cell-cycle genes to promote androgen-independent cell proliferation³³. These observations provide us with a strong rationale to utilize Eg5 inhibitors in the treatment of CRPC.

In the present study, we found a correlation between Eg5 immunohistological expression and clinicopathological characteristics, using TMAs of prostate cancer clinical specimens. Although Eg5 expression was not significantly ($P > 0.05$) associated with age, initial PSA, pathological T stage, positive surgical margin status, nor Gleason score, we did observe a significant correlation ($P = 0.004$) between Eg5 expression and Ki67 LI (the proliferation marker), which is consistent with preferential expression of Eg5 in proliferating tissues³¹. Furthermore, more than half the prostate cancer specimens showed Eg5 expression. Meanwhile, western blotting analysis showed that Eg5 expression was also present in all three prostate cancer cell

lines, LNCaP, PC3 and DU145. To summarize, Eg5 could be a potential molecular target in prostate cancer chemotherapy.

To the best of our knowledge, there have been two systematic studies involving Eg5 inhibition in prostate cancer^{34,35}. These have revealed that docetaxel-resistant and non-resistant prostate cancer cell lines showed almost the same sensitivity to antisense oligonucleotide or STLC treatment³⁴. In contrast to the antisense oligonucleotide and STLC used in those two studies, in our previous study, our target Eg5 inhibitor, S(MeO)TLC (20 μ M), was at least 10-fold more potent for inhibition of cell proliferation, and was extremely specific to Eg5, without affecting other structurally and functionally related mitotic kinesins¹⁷. Furthermore, our current study confirmed that S(MeO)TLC exhibited more efficient anti-proliferative activity compared with STLC and the other three newly synthesized agents¹⁹. Thereafter, the mechanism of cell growth inhibition in prostate cancer cell lines caused by S(MeO)TLC treatment was clarified. S(MeO)TLC exerted its anti-proliferative effect by arresting cell-cycle progression at the G2/M phase, with a distinctive monopolar spindle phenotype and a rosette-like chromosomal arrangement. Besides, the discovery of such a distinctive monopolar spindle phenotype validates the specificity of S(MeO)TLC for Eg5 inhibition and the indispensable role of Eg5 in bipolar spindle formation. Thus, cancer cell death induced by S(MeO)TLC treatment was provoked principally by prolonged mitotic arrest in a time-dependent manner.

In view of the potent anticancer efficacy of S(MeO)TLC *in vitro*, its inhibitory effect in subcutaneous xenograft tumor models was further assessed. As expected,

S(MeO)TLC displayed its significant dose-dependent antitumor efficacy *in vivo* ($P < 0.05$). In addition, the histological observation of characteristic mitotic cells with monopolar spindle phenotype suggested that S(MeO)TLC treatment resulted in an antitumor effect through induction of mitotic arrest.

In summary, Eg5 could be a good target for prostate cancer chemotherapy. We demonstrated that S(MeO)TLC, as a novel Eg5 inhibitor, exhibited significant anticancer efficacy ($P < 0.05$) in prostate cancer both *in vitro* and *in vivo*. In consideration of the robust preclinical anticancer attributes of S(MeO)TLC, we believe that S(MeO)TLC might exhibit promising clinical efficacy in prostate cancer. Further evaluations of the safety of S(MeO)TLC in prostate cancer patients and combination chemotherapy should be made before its clinical application.

Acknowledgments

This research was supported by the Targeted Proteins Research Program and Grants-in-Aid for Scientific Research from MEXT, Japan.

References

- 1 Jemal A, Siegel R, Ward E, Hao Y, Xu J, Thun MJ. Cancer statistics, 2009. *CA Cancer J Clin* 2009; 59; 225-49.
- 2 Sim HG, Cheng CW. Changing demography of prostate cancer in Asia. *Eur J Cancer* 2005; 41; 834-45.
- 3 Sternberg CN. Systemic chemotherapy and new experimental approaches in the treatment of metastatic prostate cancer. *Ann Oncol* 2008; 19 Suppl 7; vii91-5.
- 4 Petrylak DP, Tangen CM, Hussain MH, Lara PN Jr, Jones JA, Taplin ME *et al.* Docetaxel and estramustine compared with mitoxantrone and prednisone for advanced refractory prostate cancer. *N Engl J Med* 2004; 351; 1513-20.
- 5 Tannock IF, de Wit R, Berry WR, Horti J, Pluzanska A, Chi KN *et al.* Docetaxel plus prednisone or mitoxantrone plus prednisone for advanced prostate cancer. *N Engl J Med* 2004; 351; 1502-12.
- 6 Giannakakou P, Gussio R, Nogales E, Downing KH, Zaharevitz D, Bollbuck B *et al.* A common pharmacophore for epothilone and taxanes: molecular basis for drug resistance conferred by tubulin mutations in human cancer cells. *Proc Natl Acad Sci U S A* 2000; 97; 2904-9.
- 7 Geney R, Ungureanu M, Li D, Ojima I. Overcoming multidrug resistance in taxane chemotherapy. *Clin Chem Lab Med* 2002; 40; 918-25.
- 8 Mozzetti S, Ferlini C, Concolino P, Filippetti F, Raspaglio G, Prislei S *et al.* Class III beta-tubulin overexpression is a prominent mechanism of paclitaxel resistance in ovarian cancer patients. *Clin Cancer Res* 2005; 11; 298-305.
- 9 Pronk LC, Hilkens PH, van den Bent MJ, van Putten WL, Stoter G, Verweij J. Corticosteroid co-medication does not reduce the incidence and severity of neurotoxicity induced by docetaxel. *Anticancer Drugs* 1998; 9;

759-64.

- 10 Sawin KE, LeGuellec K, Philippe M, Mitchison TJ. Mitotic spindle organization by a plus-end-directed microtubule motor. *Nature* 1992; 359; 540-3.
- 11 Blangy A, Lane HA, d'Herin P, Harper M, Kress M, Nigg EA. Phosphorylation by p34cdc2 regulates spindle association of human Eg5, a kinesin-related motor essential for bipolar spindle formation in vivo. *Cell* 1995; 83; 1159-69.
- 12 Mayer TU, Kapoor TM, Haggarty SJ, King RW, Schreiber SL, Mitchison TJ. Small molecule inhibitor of mitotic spindle bipolarity identified in a phenotype-based screen. *Science* 1999; 286; 971-4.
- 13 Sakowicz R, Finer JT, Beraud C, Crompton A, Lewis E, Fritsch A *et al.* Antitumor activity of a kinesin inhibitor. *Cancer Res* 2004; 64; 3276-80.
- 14 Sawin KE, Mitchison TJ. Mutations in the kinesin-like protein Eg5 disrupting localization to the mitotic spindle. *Proc Natl Acad Sci U S A* 1995; 92; 4289-93.
- 15 Peters T, Lindenmaier H, Haefeli WE, Weiss J. Interaction of the mitotic kinesin Eg5 inhibitor monastrol with P-glycoprotein. *Naunyn Schmiedebergs Arch Pharmacol* 2006; 372; 291-9.
- 16 Marcus AI, Peters U, Thomas SL, Garrett S, Zelnak A, Kapoor TM *et al.* Mitotic kinesin inhibitors induce mitotic arrest and cell death in Taxol-resistant and -sensitive cancer cells. *J Biol Chem* 2005; 280; 11569-77.
- 17 Ogo N, Oishi S, Matsuno K, Sawada J, Fujii N, Asai A. Synthesis and biological evaluation of L-cysteine derivatives as mitotic kinesin Eg5 inhibitors. *Bioorg Med Chem Lett* 2007; 17; 3921-4.
- 18 Kozielski F, Skoufias DA, Indorato RL, Saoudi Y, Jungblut PR, Hustoft HK *et al.* Proteome analysis of apoptosis signaling by S-trityl-L-cysteine, a potent reversible inhibitor of human mitotic kinesin Eg5. *Proteomics* 2008; 8; 289-300.
- 19 Debonis S, Skoufias DA, Indorato RL, Liger F, Marquet B, Laggner C *et al.* Structure-activity relationship of

- S-trityl-L-cysteine analogues as inhibitors of the human mitotic kinesin Eg5. *J Med Chem* 2008; 51; 1115-25.
- 20 Watanabe T, Oishi S, Fujii N, Ohno H. Palladium-catalyzed direct synthesis of carbazoles via one-pot N-arylation and oxidative biaryl coupling: synthesis and mechanistic study. *J Org Chem* 2009; 74; 4720-6.
- 21 Oishi S, Watanabe T, Sawada J, Asai A, Ohno H, Fujii N. Kinesin spindle protein (KSP) inhibitors with 2,3-fused indole scaffolds. *J Med Chem* 2010; 53; 5054-8.
- 22 Ding S, Nishizawa K, Kobayashi T, Oishi S, Lv J, Fujii N *et al.* A potent chemotherapeutic strategy for bladder cancer: (S)-methoxy-trityl-L-cystein, a novel Eg5 inhibitor. *J Urol* 2010; 184; 1175-81.
- 23 Nogawa M, Yuasa T, Kimura S, Kuroda J, Sato K, Segawa H *et al.* Monitoring luciferase-labeled cancer cell growth and metastasis in different in vivo models. *Cancer Lett* 2005; 217; 243-53.
- 24 Inoue T, Segawa T, Shiraishi T, Yoshida T, Toda Y, Yamada T *et al.* Androgen receptor, Ki67, and p53 expression in radical prostatectomy specimens predict treatment failure in Japanese population. *Urology* 2005; 66; 332-7.
- 25 Prostate. In: Greene F, Page D Fleming I, eds. *American Joint Committee on Cancer Staging Manual*. 6th ed. New York: Springer; 2002. p309-316.
- 26 *General Rules for Clinical and Pathological Studies on Prostate Cancer*, 3rd ed. Japanese Urological Association, Japanese Society of Pathology, 2001.
- 27 Matsui Y, Watanabe J, Ding S, Nishizawa K, Kajita Y, Ichioka K *et al.* Dicoumarol enhances doxorubicin-induced cytotoxicity in p53 wild-type urothelial cancer cells through p38 activation. *BJU Int* 2010; 105; 558-64.
- 28 Inoue T, Yoshida T, Shimizu Y, Kobayashi T, Yamasaki T, Toda Y *et al.* Requirement of androgen-dependent activation of protein kinase Czeta for androgen-dependent cell proliferation in LNCaP Cells and its roles in transition to androgen-independent cells. *Mol Endocrinol* 2006; 20; 3053-69.

- 29 Schmidt M, Bastians H. Mitotic drug targets and the development of novel anti-mitotic anticancer drugs. *Drug Resist Updat* 2007; 10; 162-81.
- 30 Jackson JR, Patrick DR, Dar MM, Huang PS. Targeted anti-mitotic therapies: can we improve on tubulin agents?. *Nat Rev Cancer* 2007; 7; 107-17.
- 31 Hegde PS, Cogswell J, Carrick K, Jackson J, Wood KW, Eng WK, Brawner M, Huang PS, Bergsma D. Differential gene expression analysis of kinesin spindle protein in human solid tumors. *Proc Am Soc Clin Oncol* 2003; 22; 535.
- 32 Nakai R, Iida S, Takahashi T, Tsujita T, Okamoto S, Takada C *et al.* K858, a novel inhibitor of mitotic kinesin Eg5 and antitumor agent, induces cell death in cancer cells. *Cancer Res* 2009; 69; 3901-9.
- 33 Wang Q, Li W, Zhang Y, Yuan X, Xu K, Yu J *et al.* Androgen receptor regulates a distinct transcription program in androgen-independent prostate cancer. *Cell* 2009; 138; 245-56.
- 34 Wiltshire C, Singh BL, Stockley J, Fleming J, Doyle B, Barnetson R *et al.* Docetaxel-Resistant Prostate Cancer Cells Remain Sensitive to S-Trityl-L-Cysteine-Mediated Eg5 Inhibition. *Mol Cancer Ther* 2010.
- 35 Hayashi N, Koller E, Fazli L, Gleave ME. Effects of Eg5 knockdown on human prostate cancer xenograft growth and chemosensitivity. *Prostate* 2008; 68; 1283-95.

Figure 1.

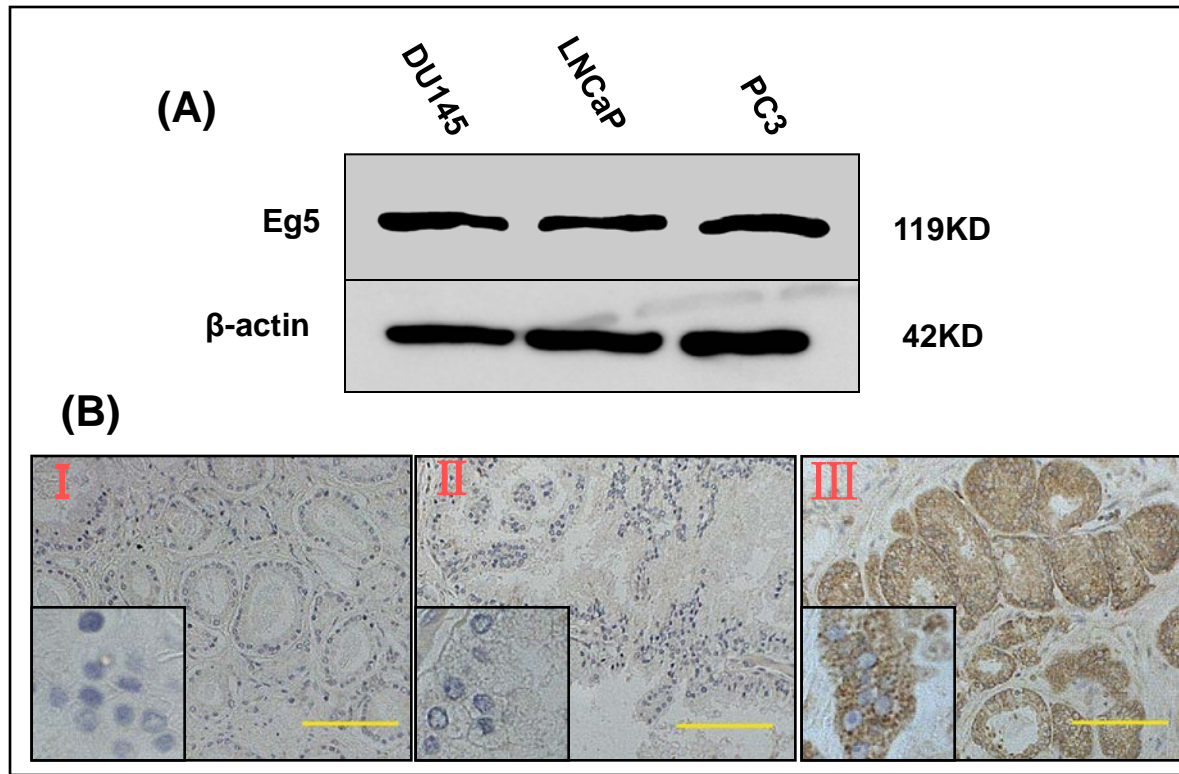


Figure 2.

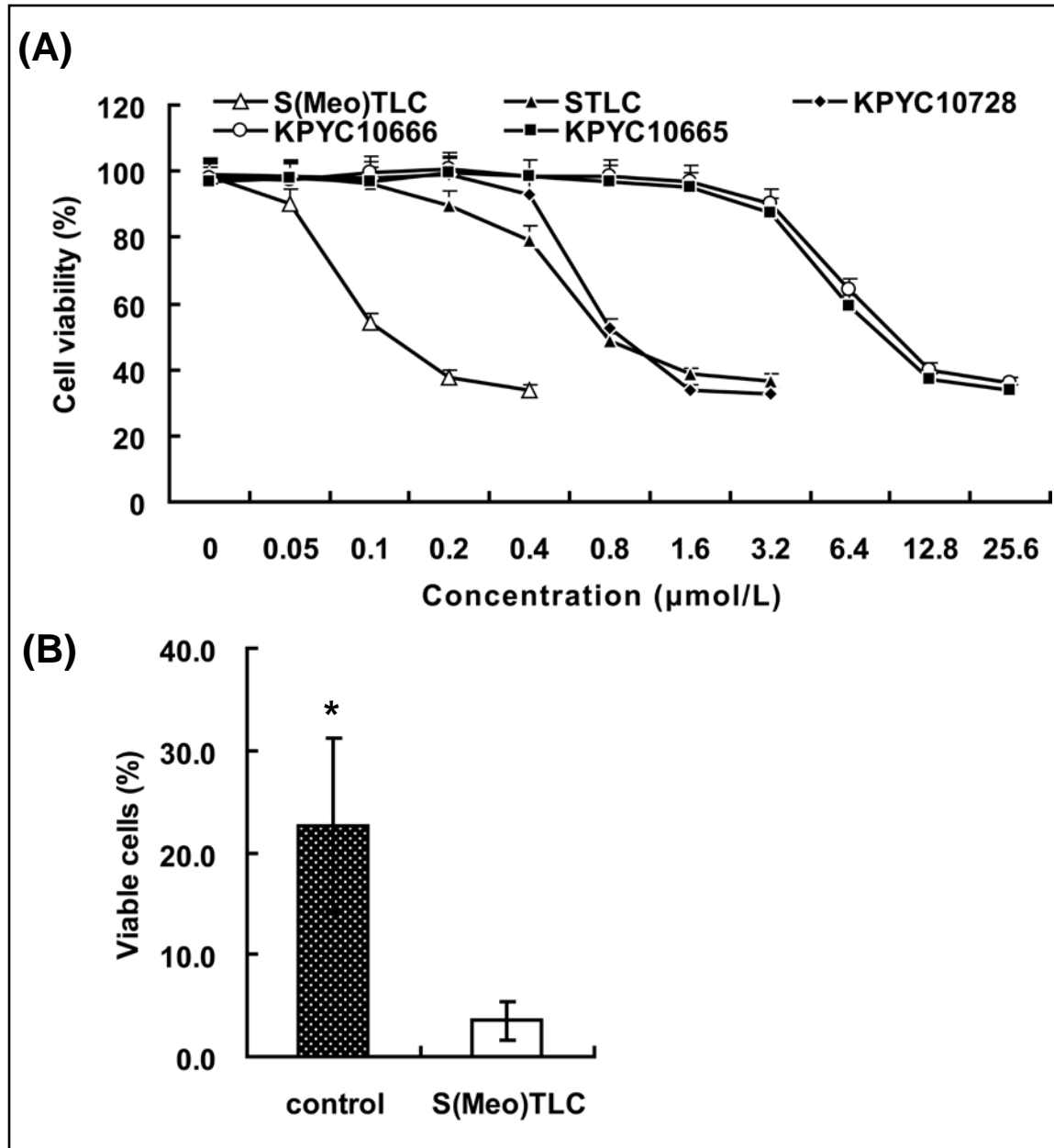


Figure 3.

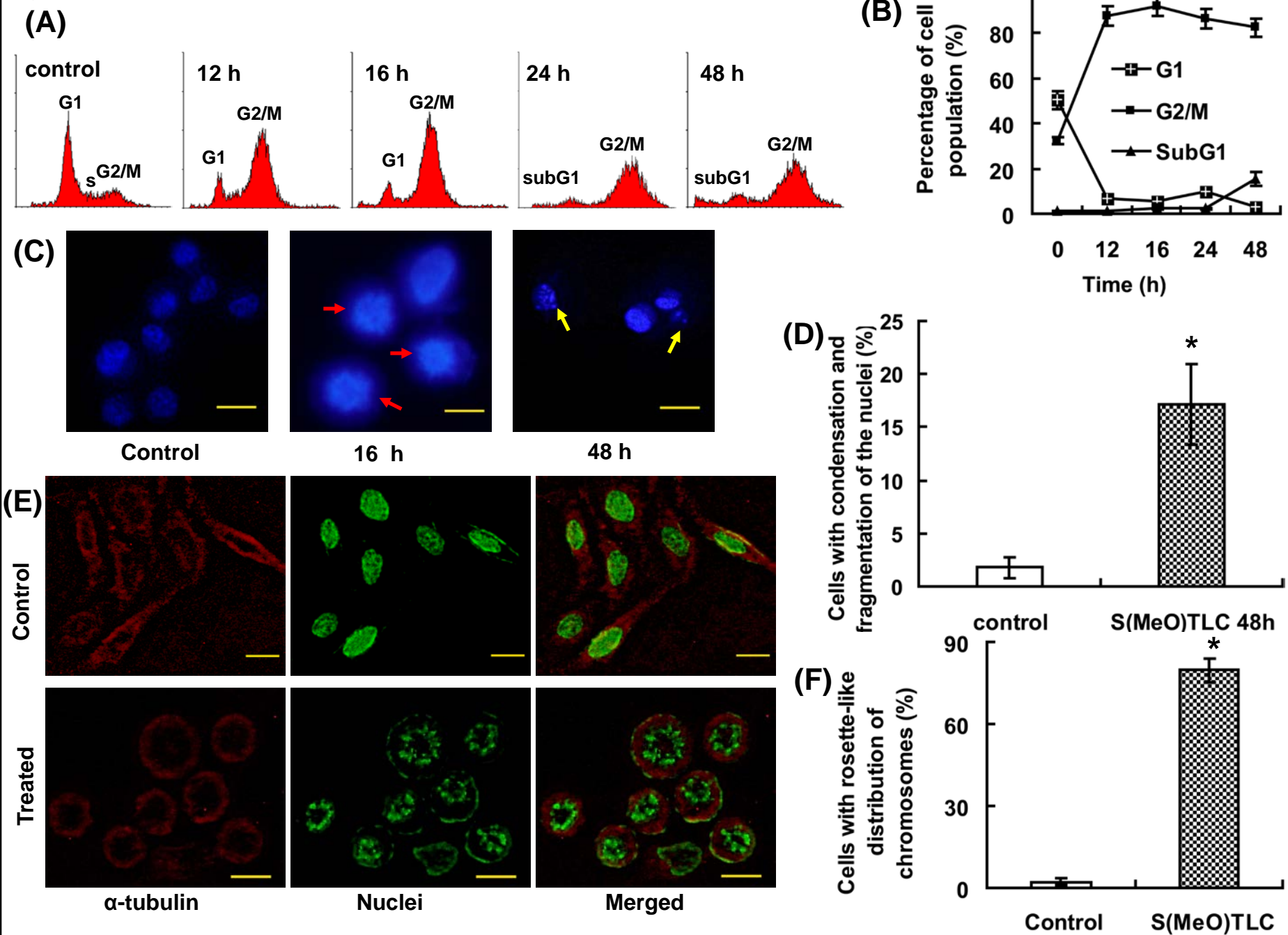


Figure 4.

